Geosci. Instrum. Method. Data Syst. Discuss., https://doi.org/10.5194/gi-2018-43
Manuscript under review for journal Geosci. Instrum. Method. Data Syst.
Discussion started: 3 December 2018

Geoscientific Instrumentation Methods and Data Systems Open Access Discussions

Continuous observation of Stable Isotopes of Water Vapor in Atmosphere Using High-Resolution FTIR

Chang-gong Shan [1, 2], Wei Wang [2*], Cheng Liu [2,3,4*], You-wen Sun[2], Yuan Tian[2], Isamu Morino[5]

[1]School of Environment science and Optoelectronic Technology, University of Science and Technology of China, Hefei, 230000, China

[2] Key Laboratory of Environmental Optics and Technology, Anhui Institute of Optics and Fine Mechanics, Chinese Academy of Sciences, Hefei, 230031, China

[3] University of Science and Technology of China, Hefei, 230000, China

[4]Center for Excellence in Urban Atmospheric Environment, Institute of Urban Environment, Chinese Academy of Sciences, Xiamen, 361021, China

[5]Satellite Observation Center, National Institute for Environmental Studies, Tsukuba, 305-8506, Japan

Correspondence to: Cheng Liu (chliu81@ustc.edu.cn),
Wei Wang (wwang@aiofm.ac.cn)

Abstract

Observations of stable isotopes of water vapor provide important information for water cycle. The volume mixing ratios (VMR) of H_2O (X_{H2O}) and HDO (X_{HDO}) have been retrieved based on a high-resolution ground-based Fourier transform infrared spectroscopy (FTIR) at Hefei site, and the isotopic composition δD was calculated. Time series of X_{H2O} were compared with the Greenhouse gases Observing Satellite (GOSAT) data, showing a good agreement. The daily averaged δD ranges from -17.02‰ to -282.3‰ between September 2015 and September 2016. Also, the relationships of meteorological parameters with stable isotopologue were analyzed. δD values showed an obvious positive correlation with temperature and ln(X_{H2O}) and a weak correlation with relative humidity. Further, 51.35% of airmass at Hefei site comes from the southeast of China, and the main potential sources of δD are in the east of China over the observation period based on the back trajectories model. Furthermore, the δD values of evapotranspiration were calculated based on Keeling plot. Observations of the stable isotopes of water vapor by high-resolution ground-based FTIR provide information on study of the variation of the atmospheric water vapor at Hefei site.

1. Introduction

Water cycle plays an important role in climate change. Water vapor plays a key role in cloud formation progress, however, its associated feedback mechanism is poorly known (Soden et al., 2005; Boucher et al., 2013). Observations of stable isotopes of water vapor in the atmosphere provide important information for hydrological cycle, because the stable isotopes change with the phase change of water vapor. The variation of stable isotopes of water vapor in the atmosphere reflects the change of water cycle, and the measurements of stable isotopes reveal the relationship between atmospheric dynamics, evaporation, and condensation process (Yoshimura et al., 2008; Risi et al., 2010).

The stable isotopologues of water vapor mainly include $H_2{}^{16}O$, HDO and $H_2{}^{18}O$. The HDO/H_2O ratio is usually expressed as a ratio of HDO to H_2O abundance. The "delta notation" is usually used to represent the isotopic composition, and normally defined as:

$$\delta D = \left(\frac{R_m}{R_s} - 1\right) \times 1000‰ \quad (1)$$

Where R_s (equals to 3.1152×10^{-4}) is the standard HDO abundance of Vienna standard mean ocean water (VSMOW), and R_m is the measured ratio of HDO/H_2O (Craig et al., 1961).

Water vapor mainly exists in the troposphere, more than 60 % of water vapor are below 850 hPa and 90 % below 500 hPa (Ross et al., 1996). Gribanov (2014) proved that the column averaged HDO/H_2O ratio is highly correlated with near surface δD. Recent studies used column averaged HDO/H_2O ratio combined with in-situ δD measurements to study the seasonal and inter-seasonal variations of water cycle (Gribanov et al., 2014). The variation of atmospheric temperature and humidity near the surface also cause the atmospheric water recycling (Boucher et al., 2004; Destouni et al., 2010; Tuinenburg et al., 2012). Therefore, many studies reported that meteorological parameters at ground level are correlated with the stable isotopologue of water vapor. For example, δD have a positive correlation with temperature and relative humidity of the atmosphere in summer in Mediterranean coastal area (Delattre et al., 2015). Bastrikov (2014) also analyzed the relationship between δD and temperature and humidity in different seasons in West Siberia. However, these reports are based on in-situ measurements, and there are few studies about the relationship between the column averaged HDO/H_2O

ratio δD and the meteorological parameters.

Ground-based FTIR technique is widely used to obtain long-term time series of atmospheric composition and validate satellite data (Schneising et al., 2012; Scheepmaker et al., 2015). High-resolution FTIR observations have achieved accurate detection of greenhouse and trace gases (Washenfelder et al., 2006). The Total Carbon Column Observing Network (TCCON) and the Network for the Detection of Atmospheric Composition Change (NDACC) use high-resolution FTIR instrument to accurately and precisely derive the main stable isotopologue of water vapor, HDO (Hannigan et al., 2009; Wunch et al., 2011). The total column of HDO and H_2O are retrieved in the near infrared region, and the column averaged HDO/H_2O ratio are calculated. Also, the Column averaged HDO derived from the high-resolution FTIR instrument have been used for comparison with model simulations and satellite data (Boesch et al., 2013; Frankenberg et al., 2013; Rokotyan et al., 2014; Dupuy et al., 2016).

Water isotopologues composition has been analyzed in Hefei with an obvious seasonal variation, only at the month scale, using in situ measurements (Wang et al., 2012). However, so far no research has been dedicated to the water vapor and its isotopologues variation in a large spatial-temporal scale at Hefei. To better understand evapotranspiration, process and the relationship between meteorological parameters and water vapor isotopologues, the column stable isotopologues of water vapor observed by ground-based FTIR technique are presented in the paper.

The instrumentation and retrieval strategy for column averaged H_2O and HDO at Hefei site are described in Section 2. The retrieval results are discussed in Section 3, also, the relationships between the isotopic composition δD and temperature, relative humidity are analyzed. Moreover, the evapotranspiration signature δ_{ET} and the sources of water vapor based on the back trajectories calculation of air masses are clarified in this Section. The conclusions are given in Section 4.

2. Instrumentation and retrieval strategy

The ground-based high-resolution FTIR spectrometer (Bruker IFS 125 HR) and solar

Geosci. Instrum. Method. Data Syst. Discuss., https://doi.org/10.5194/gi-2018-43
Manuscript under review for journal Geosci. Instrum. Method. Data Syst.
Discussion started: 3 December 2018

Geoscientific Instrumentation Methods and Data Systems Discussions

tracker (A547) installed on the roof of laboratory, are combined to collect the solar absorption spectra at Hefei site. Hefei (31.9 °N, 117.17 °E, about 30 m above the sea level) is a continental site, away from the southeast urban area about 10 km (Figure 1). The CaF_2 beamsplitter and InGaAs detector are used to collect the near-infrared (NIR) spectra. The NIR spectral range covers 4000-11000cm^{-1}, and the spectral resolution is 0.02 cm^{-1}, corresponding to a 45 cm maximum optical path. In order to ensure the stability of the measurement, the instrument is vacuated under 10 hPa. A weather station is installed near the solar tracker on the roof of the lab building to record meteorological data. Wang (2017) described the instrumentation and the measurement routine at Hefei site.

The solar spectra collected from September 2015 to September 2016 are analyzed. We use the GGG2014 software package to retrieve the water vapor and its isotopes (Wunch et al., 2015). GGG2014 is a nonlinear least square spectral fitting algorithm (GFIT), which scales an a priori profile derived from the National Centers for Environmental Prediction and the National Center for Atmospheric Research (NCEP/NCAR) reanalysis data (Toon et al., 2014) to minimize residulas between measured and simukated spectra. GGG2014 produces the total column of trace gases, then the column-averaged dry-air mole fractions (DMF) of trace gasees are computed as:

$$X_{gas} = \frac{column_{gas}}{column_{air}^{dry}}$$

$$= 0.2095 \times \frac{column_{gas}}{column_{O_2}} \quad (2)$$

The column of dry air, units of molecules/cm^2, is computed from the oxygen (O_2) column (Wunch et al, 2011) dividing by 0.2095. Figure 2 depicts the spectral fitting of the H_2O and HDO in the spectral window of 4565-6470 and 4054-6400 cm^{-1}, respectively. The rms spectral fitting residuals are 0.16% and 0.25% for H_2O and HDO respectively. Table 1 lists the spectral windows for column retrievals of H_2O and HDO, which are the standard GFIT windows. Figure 3 shows the column averaging kernals of H_2O and HDO. The difference of the column averaging kernals below 500 hPa between them is very small, with the value of 4.34%.

3. Results

3.1. Time series of δD, water vapor and meteorological parameters

The DMFs of H_2O and HDO are calculated using total columns of H_2O and HDO based on equation (2). The δD time series at Hefei station is plotted in Figure 4 from September 2015 to September 2016. The precision of δD (1-σ precision divided by the measured value) is about 3.63%. The daily averaged δD varies from -17.02‰ to -282.3‰. δD shows an obvious seasonal variation over the observed period, with the lowest δD values occurring in mid-January and the peak in early August.

The time series of X_{H2O} and meteorological parameters from September 2015 to September 2016 at Hefei station are plotted in Figure 5. The mean relative retrieval error (1-σ precision divided by the measured value) of X_{H2O} is about 1.11%. The variations of X_{H2O} are similar to those of δD, with an obvious seasonal pattern. The variation of X_{H2O} is large during the period. The daily averaged X_{H2O} was in the peak of 8821.97 ppm in early August in summer and reduced to the minimum of 225 ppm in mid-January in winter. The variation of surface temperature is close to X_{H2O} variation, while the relative humidity of atmosphere shows a weak seasonal variation. The peak and valley values of water vapor and δD seem to accompany with those of temperature, and the different amplitude of daily variation of δD in different seasons depends on temperature, therefore, the relationships of water vapor and δD with temperature are discussed in sec.4.2.

4. Discussion

4.1 Comparison with nearby TCCON observations and satellite data

The time series of X_{H2O} are compared with the GOSAT data (v02.72) from September 2015 to September 2016. For co-locating the GOSAT data with the ground-based FTS data, the GOSAT observations of $\pm 5°$ latitude and longitude centered in the Hefei site within ± 2 hour overpass were selected (Kuze et al., 2009; Yoshida et al., 2013; Scheepmaker et al., 2015). In order to eliminate the influence of different a priori profiles and averaging kernels on X_{H2O}, we use a priori profile of the ground-based FTS to correct the column-averaged mole fractions of gases from GOSAT (Reuter et al., 2011; Zhou et al., 2016). The comparison results of X_{H2O} are depicted in Figure 6. The mean bias, which is defined as the mean difference of X_{H2O} between FTIR and satellite date, is about 11.98ppm. The X_{H2O} observed by FTIR showed a similar variation trend with the corrected satellite data, and the variation range agrees with that of GOSAT data. Since water vapor mainly concentrate in the lower troposphere, and the ground-based observations have high sensitivity near surface, but the satellite data are insensitive in the lower troposphere, so the FTIR data are slightly higher than the satellite data. Also, we calculated the correlation between FTIR and GOSAT data, and there is a high correlation between FTIR and GOSAT data (R = 0.98). The correlation coefficients between FTIR and GOSAT data are 0.95 and 0.93 for Japanese Tsukuba and Saga site, respectively (Dupuy et al.; 2016). The slope of the scatter plot of our FTIR and GOSAT data is 0.98. It is concluded that FTIR data at Hefei site agree well with the satellite observations.

Furthermore, to verify the accuracy of our calculated data, we compare the isotopic ratios δD from Tsukuba TCCON station (Morino et al., 2014) with our δD values. Tsukuba TCCON station (36.05°N, 140.12°E, 31m above the sea level) is a Japanese TCCON station close to our site and at a similar latitude (Figure 1). Figure 7 is the plot of δD in Hefei compared to those of Tsukuba from September 2015 to February 2016. It is found that the δD in Hefei showed a similar trend as that in Tsukuba, both with the maximum value in summer and the minimum in winter. During the observation period, the δD of the two sites began to fall from October 2015 and to the valley value in January 2016. Hefei and Tsukuba sites have a similar atmosphere circulation pattern due to the similar latitude, which may result in the similar variation in the stable isotopes of water vapor in the atmosphere, as shown in Figure 7. However, the daily averaged δD of Hefei ranges from -36.46‰ to -282.3‰ during this period, while δD in Tsukuba is from -35.74‰ to -198.37‰, falling in the range of our δD. Scheepmaker (2015) plots the time series of δD in six TCCON stations, and the δD observed from these stations in the Northern hemisphere are in the range from about -50‰ to -300‰, which are comparable to those of our results.

Geosci. Instrum. Method. Data Syst. Discuss., https://doi.org/10.5194/gi-2018-43
Manuscript under review for journal Geosci. Instrum. Method. Data Syst.
Discussion started: 3 December 2018

Geoscientific Instrumentation Methods and Data Systems Discussions

4.2. Relationship of stable isotopes of water vapor with meteorological parameters

Atmospheric circulation strongly affects the variations of stable isotopic compositions of water vapor in the atmosphere (Deshpande et al., 2010; Guan et al., 2013). The spatiotemporal distribution of water vapor in the atmosphere is strongly correlated with the weather, and the stable isotopic ratios of water vapor change with the meteorological parameters (Noone et al., 2012, Vogelmann et al., 2015). The surface meteorological data are important for quantifying the distributions of the stable isotopes of water vapor. The statistical data of monthly averaged δD and surface temperature are summarized in Table 1. The monthly averaged surface temperature decreased from 30.18 to 4.74 ℃ between Sep.2015 and Jan.2016, and the variation of δD also dropped from -126.89‰ to -257.86‰ at the same time. Especially, the daily averaged δD reached the minimum of -282.3‰ in 25 January 2016, which is the coldest day during the period. Also, δD shows a large variation in winter, with the monthly variation amplitude of 186.38‰ and 213.66‰ in December 2015 and February 2016, respectively. However, the monthly variation amplitude of δD in summer is about one third of the corresponding values in winter. Furthermore, the monthly variation amplitude of temperature is 14.1 and 19.2℃ in December 2015 and February 2016, respectively, while the corresponding value is 6.3 and 8℃ in July and August, respectively. It is noted that the correlation coefficient between monthly variation amplitude of δD and temperature is 0.95. So it is concluded that the surface temperature strongly influences the variation of δD in Hefei site.

For all the data collected, the linear relationship of individual δD and the surface temperature is expressed as δD=5.30‰T-242.64‰. The correlation coefficient is 0.83 between δD and temperature at Hefei site, as shown in Figure 8(a). Bastrikov (2014) and Bonne (2014) found that there was a positive correlation between the stable isotopes of water vapor and temperature in western Siberia and southern Greenland. In Bastrikov (2014), the slope of δD and temperature in western Siberia is 3.1‰℃$^{-1}$. The evaporation of water vapor weakens with the decrease of temperature, and heavier isotopologue, HDO, condenses more actively and evaporate less actively than the main isotopologue H_2O due to their different saturation vapor pressure, so the depletion in heavy isotopes with decreasing temperature happens.

Geosci. Instrum. Method. Data Syst. Discuss., https://doi.org/10.5194/gi-2018-43
Manuscript under review for journal Geosci. Instrum. Method. Data Syst.
Discussion started: 3 December 2018

Geoscientific Instrumentation Methods and Data Systems
Open Access
Discussions

δD of atmosphere in Hefei show a weak correlation with relative humidity, as plotted in Figure 8(b). The correlation coefficient of linear regression between δD and relative humidity is 0.45, and the slope of linear regression is 2.11‰$\%^{-1}$. Wen (2010) reported that the stable isotopes of water vapor in Beijing is positively correlated with the relative humidity (R = 0.42), while the diurnal and seasonal variation of δD have a strong relationship with the relative humidity in northwest Greenland (Steen-Larsen et al., 2013).

A simple distillation model, Rayleigh distillation model, helps to understand the relationship between δD and H_2O (Schneider et al., 2010). The variation of water vapor and δD are connected via the equation

$$\delta D \times 1000 = (1 + \delta D_0) \times \left(\frac{XH_2O}{XH_2O_0}\right)^{\alpha-1} - 1 \qquad (3)$$

In which δD_0 and XH_2O_0 are the deuterium and water vapor of the airmass from the ocean, while α represents the fractionation coefficient between the oceanic source and the sampling site.

There is a linear relationship between ln(δD/1000+1) and ln(X_{H2O}) , according to the equation (3). The slope of ln(δD/1000+1) and ln(X_{H2O}) represents a measure of the transport pathway of water vapor. Analysis of the slope allows investigating the importance of different hydrological processes (Worden et al., 2007; Schneider et al., 2010). As shown in Figure 8(c), there is a strong correlation (R=0.88) between ln(δD/1000+1) and ln(X_{H2O}), and the slope of linear regression is 0.081. The results prove that the stable isotopes of water vapor are highly correlated with the fraction of water remaining in the cloud. In western Siberia, the correlation coefficient of linear regression between ln(δD/1000+1)/ln(X_{H2O}) is 0.71, and the slope of linear regression is 0.07 (Gribanov et al, 2014).

4.3. Variation sources of regional δD in Hefei

The NOAA Hybrid Single-Particle Lagrangian Integrated Trajectory (HYSPLIT) model is a complete system using NCEP/NCAR reanalysis data to understand transport paths and sources of air masses (Draxler and Rolph, 2003; Stein et al., 2015). The HYSPLIT model is used to analyze the Potential Sources Contribution Function (PSCF)

Geosci. Instrum. Method. Data Syst. Discuss., https://doi.org/10.5194/gi-2018-43
Manuscript under review for journal Geosci. Instrum. Method. Data Syst.
Discussion started: 3 December 2018

of air parcels (Li et al., 2012). The back trajectories of 72 hours are calculated for each day, and the height of the backward trajectories is set as 500 magl. The geographic region precision is selected as 0.5°× 0.5° grid cells in the calculation. The PSCF calculated by the backward trajectories is weighted according to the method of Polissar et al. (1999) to identify the source strength (WPSCF).

Figure 9 shows the cluster analysis results and the WPSCF distribution of δD during the period from September 2015 to August 2016. The sources of air masses of Hefei area mainly originated from three regions: the Southeast China (SEC), North of China (NC) and Northwest of China (NWC). 51.35% of airmass were from SEC during the observation period. Also, The WPSCF analysis indicates that the main potential sources of δD are near the Hefei site. The potential source of δD are divided into three regions: the east area with moist and warm airmass, the north area with dry and cold airmass, and the southwest area with moist and warm airmass. Especially the main airmass from the east area bring the moist and warm airmass into Hefei, which result in the enrichment of heavy isotopes.

4.4 δ-value of evapotranspiration

Keeling plot is usually applied to estimate the δ-value of evapotranspiration (Keeling et al., 1958; Wei et al., 2015). The Keeling equation assumes that the actual atmospheric water vapor is the mixing of the atmospheric background and an additional component from local evapotranspiration, and each component has distinct isotopic signature. The water vapor and its isotopes in the atmosphere can be written as (Yepez et al., 2003; Williams et al., 2004; Sun et al., 2005)

$$\delta_m = (\delta_b - \delta_{ET})W_b\left(\frac{1}{W_m}\right) + \delta_{ET} \quad (4)$$

Where W_m and δ_m are DMF and δ-value of the water vapor, respectively. W_b and δ_b are DMF and δ-value of the background, respectively. δ_{ET} is the δ-value of evapotranspiration. Therefore, the evapotranspiration signature (δ_{ET}) is also expressed as the y-axis intercept of equation (4).

Keeling plot is used to calculate the δ-value of the evapotranspiration of water vapor. The days with 4-hour continuous observations are considered to ensure that the data are representative. The δD and $1/X_{H2O}$ have a high-negative correlation in daily timescale, as shown in Figure 10. The correlation coefficients are -0.97 and -0.85, and the y-axis intercepts of the linear regression line represent the δD from evapotranspiration source of water vapor, which are -35.39 ‰ and -53.18 ‰ for October 27, 2015 and December 17, 2015, respectively. The time series of δD for evapotranspiration obtained from keeling plot analysis during the measurement period are shown in Figure 11. Over the period, δD value of evapotranspiration varied from (15.3 ± 2.9) ‰ to (-114 ± 8.9) ‰, and the averaged δD value of evapotranspiration is -44.43 ‰. It is seen that the variation range of δ D value for evapotranspiration was large, reflecting the fact that the source isotopic signal did not keep constant over the measurement period. In the study of Wang (2012), the deuterium isotopic signature from evapotranspiration is between -113.93 ± 10.25 ‰ and -245.63 ± 17.61 ‰ in July in Hefei. Griffith (2006) found that the deuterium isotopic ratio from evapotranspiration is between -90 ‰ and -100 ‰ in a pasture.

5. Conclusions

The DMFs of H_2O and HDO were retrieved from the spectra observed by the ground-based high resolution FTIR at Hefei site. Time series of X_{H2O} were compared with GOSAT data. The mean relative bias was 2.85% and the correlation coefficient is 0.98 between FTIR and satellite date, showing a good agreement. X_{HDO}/X_{H2O} ratio expressed as δD are calculated. δD from nearby Tsukuba station with similar latitude are used to verify the accuracy of our data. It is found that the δD in Hefei showed a same trend as that in Tsukuba, with the maximum value in summer and minimum in winter. Variation of δD ranges from -36.46‰ to -282.3‰, while δD in Tsukuba is from -35.74‰ to -198.37‰.

The relationship of meteorological parameters with stable isotopes of water vapor were analyzed. The δD values and temperature showed an obvious positive correlation, with the correlation coefficient of 0.83, while δD has weak correlation with relative humidity, with the correlation coefficient of 0.45. ln(δD*1000+1) has obvious correlation with $\ln(X_{H2O})$, with the correlation coefficient of 0.88.

Further, we used the NOAA HYSPLIT model to calculate the back trajectories of air parcels in Hefei, and performed the cluster analysis and PSCF analysis. The results of cluster and PSCF analysis showed the sources of δD and their potential contributions are mainly from the surrounding area of Hefei site and especially in the east area. Also, the δD value of evapotranspiration is calculated based on Keeling plot analysis. δD value of evapotranspiration varied from (15.3 ± 2.9) ‰ to (-114 ± 8.9) ‰, and the averaged δD value of evapotranspiration is -44.43‰.

The FTIR technique offers a new opportunity to monitor the stable isotopes of water vapor. The long time series of the stable isotopes of water vapor provide a basis of revealing the water cycle of the atmosphere. The further research work will focus on accurate retrieval of $H_2{}^{18}O$ from solar absorption spectra, and can clearly clarify the water cycle in combination with HDO.

Data availability. The **GFIT** software can be found via https://tccon-wiki.caltech.edu/. The data used in this paper are available on request.

Funding sources and acknowledgments.

We gratefully acknowledge the support of the National Natural Science Foundation of China (41775025; 41405134; 41575021; 91544212; 41605018), the National Key Technology R&D Program of China (2017YFC0210002; 2016YFC0200800; 2016YFC0200404; 2016YFC0203302), and Anhui Province Natural Science Foundation of China (Grant No. 1308085MD79) for conducting this research. We thank the NIES GOSAT Project Office for the GOSAT TANSO-FTS SWIR X_{H2O} data. The authors gratefully acknowledge the NOAA Air Resources Laboratory (ARL) for providing the HYSPLIT transport model (http://ready.arl.noaa.gov/HYSPLIT.php).

References

Bastrikov, V., Steen-Larsen, H. C., Masson-Delmotte, V., Gribanov, K., Cattani, O., Jouzel, J., and Zakharov, V.: Continuous measurements of atmospheric water vapour isotopes in western Siberia (Kourovka), Atmos. Meas. Tech., 2014, 7, 1763–1776, doi:10.5194/amt-7-1763-2014, 2014.

Boesch, H., Deutscher, N. M., Warneke, T., Byckling, K., Cogan, A. J., Griffith, D. W. T., Notholt, J., Parker, R. J., and Wang, Z.: HDO/H2O ratio retrievals from GOSAT, Atmos. Meas. Tech., 2013, 6, 599–612, doi:10.5194/amt-6-599-2013, 2013.

Bonne, J.-L., Masson-Delmotte, V., Cattani, O., Delmotte, M., Risi, C., Sodemann, H., and Steen-Larsen, H. C.: The isotopic composition of water vapour and precipitation in Ivittuut, southern Greenland, Atmos. Chem. Phys., 2014, 14, 4419–4439, doi:10.5194/acp-14-4419-2014, 2014.

Boucher O, Myhre G, and Myhre A. Direct human influence of irrigation on atmospheric water vapour and climate. Climate Dynamics, 2004, 22(6):597-603.

Boucher, O., Randall, D., Artaxo, P., Bretherton, C., Feingold, G., Forster, P., Kerminen, V.-M., Kondo, Y., Liao, H., Lohmann, U., Rasch, P., Satheesh, S. K., Sherwood, S., Stevens, B., and Zhang, X. Y.: Clouds and aerosols, in: Climate Change 2013: The Physical Science Basis. Contribution of Working Group I to the Fifth Assessment Report of the Intergovernmental Panel on Climate Change, edited by: Stocker, T. F., Qin, D., Plattner, G.-K., Tignor, M., Allen, S. K., Doschung, J., Nauels, A., Xia, Y., Bex, V., and Midgley, P. M.: Cambridge Universit Press, United Kingdom and New York USA, 571–657, doi:10.1017/CBO9781107415324.016, 2013.

Craig H. Standard for Reporting Concentrations of Deuterium and Oxygen-18 in Natural Waters. Science, 1961, 133(3467):1833-4.

Delattre H, Valletcoulomb C, and Sonzogni C. Deuterium excess in the atmospheric water vapour of a Mediterranean coastal wetland: regional vs. local signatures. Atmospheric Chemistry & Physics, 2015, 15(2015):10167-10181.

Deshpande, R. D., A. S. Maurya, B. Kumar, A. Sarkar, and S. K. Gupta. Rain-vapor interaction and vapor source identification using stable isotopes from semiarid western India. Journal of Geophysical Research-Atmospheres 2010, 115(115):6696-6705.

Destouni G, Asokan S M, and Jarsjö J. Inland hydro-climatic interaction: effects of human water use on regional climate. Geophysical Research Letters, 2010, 37(18):389-390.

Draxler, R.R., Rolph, G.D., 2003. HYSPLIT (HYbrid Single-particle Lagrangian Integrated Trajectory). NOAA Air Resources Laboratory, Silver Spring, MD. http://www.arl.noaa.gov/ready/hysplit4.html.

Dupuy, E., Morino, I., Deutscher, N., Yoshida, Y., Uchino, O., Connor, B., De Mazière, M., Griffith, D., Hase, F., Heikkinen, P., Hillyard, P., Iraci, L., Kawakami, S., Kivi, R., Matsunaga, T., Notholt, J., Petri, C., Podolske, J., Pollard, D., Rettinger, M., Roehl, C., Sherlock, V., Sussmann, R., Toon, G., Velazco, V., Warneke, T., Wennberg, P., Wunch, D., and Yokota, T. Comparison of X_{H2O} Retrieved from GOSAT Short-Wavelength Infrared Spectra with Observations from the TCCON Network, Remote Sens., 8, 414, doi:10.3390/rs8050414, 2016.

Frankenberg C, Wunch D, Toon G, Risi C., Scheepmaker R., Lee J.-E, and Worden J. Water vapor isotopologues retrievals from high resolution GOSAT short-wave infrared spectra[J]. Atmospheric Measurement Techniques, 2013, 6(5):263-274.

Gribanov, K., Jouzel, J., Bastrikov, V., Bonne, J.-L., Breon, F.-M., Butzin, M., Cattani, O., Masson-Delmotte, V., Rokotyan, N., Werner, M., and Zakharov, V. Developing a western Siberia reference site for tropospheric water vapour isotopologue observations obtained by different techniques (in situ and remote sensing). Atmospheric Chemistry and Physics, 2014, 14(12): 5943-5957.

Griffith, D., Jamie, I., Esler, M., Wilson, S., Parkes, S., Waring, C., and Bryant, G. Real-time field measurements of stable isotopes in water and CO_2 by Fourier transform infrared spectrometry. Isotopes in Environmental Health Studies, 2006, 42(1):9-20.

Guan HD, Zhang XP, Skrzypek G, Sun ZA, and Xu X. Deuterium excess variations of rainfall events in a coastal area of South Australia and its relationship with synoptic weather systems and atmospheric moisture sources. Journal of Geophysical Research Atmospheres, 2013, 118(2):1123-1138.

Hannigan J W, Coffey M T, and Goldman A. Semiautonomous FTS Observation System for Remote Sensing of Stratospheric and Tropospheric Gases. Journal of Atmospheric & Oceanic Technology, 2010, 26(9):1814.

Geosci. Instrum. Method. Data Syst. Discuss., https://doi.org/10.5194/gi-2018-43
Manuscript under review for journal Geosci. Instrum. Method. Data Syst.
Discussion started: 3 December 2018

Geoscientific Instrumentation Methods and Data Systems
Open Access
Discussions

Keeling C D. The concentration and isotopic abundances of atmospheric carbon dioxide in rural areas. Geochimica Et Cosmochimica Acta, 1958, 13(4):322-334.

Kuze A, Suto H, Shiomi K, Nakajima M, and Hamazaki T. On-orbit performance and level 1 data processing of TANSO-FTS and CAI on GOSAT[C]// SPIE Europe Remote Sensing. International Society for Optics and Photonics, 2009:173-183.

Li, M.M., Huang, X., Zhu, L., Li, J.F., Song, Y., Cai, X.H., Xie, S.D., 2012. Analysis of the transport pathways and potential sources of PM10 in Shanghai based on three methods. Sci. Total Environ. 414, 525–534.

Morino, I., Uchino, O., Inoue, M., Yoshida, Y., Yokota, T., Wennberg, P. O., Toon, G. C., Wunch, D., Roehl, C. M., Notholt, J., Warneke, T., Messerschmidt, J., Griffith, D. W. T., Deutscher, N. M., Sherlock, V., Connor, B., Robinson, J., Sussmann, R., and Rettinger, M. TCCON data from Tsukuba, Ibaraki, Japan, 120HR, Release GGG2014R0. TCCON data archive, hosted by the Carbon Dioxide Information Analysis Center, Oak Ridge National Laboratory, Oak Ridge, Tennessee, USA.

Noone D. Pairing measurements of the water vapor isotope ratio with humidity to deduce atmospheric moistening and dehydration in the tropical midtroposphere. Journal of Climate, 2012, 25(13): 4476-4494.

Polissar, A. V., P. K. Hopke, P. Paatero, Y. J. Kaufmann, D. K. Hall, B. A. Bodhaine, E. G. Dutton, and J. M. Harris, The aerosol at Barrow, Alaska: Long-term trends and source locations, Atmos. Environ., 33, 2441 – 2458, 1999.

Reuter, M., Bovensmann, H., Buchwitz, M., Burrows, J., Connor, B. J., Deutscher, N. M., Griffith, D. W. T., Heymann, J., Keppel-Aleks, G., Messerschmidt, J., Notholt, J., Petri, C., Robinson, J., Schneising, O., Sherlock V., Velazco V., Warneke T., Wennberg P. O., and Wunch, D., Retrieval of atmospheric CO2 with enhanced accuracy and precision from SCIAMACHY: Validation with FTS measurements and com-parison with model results, J. Geophys. Res., 2011, 116, D04301, doi:10.1029/2010JD015047, 2011.

Risi, C., Bony, S., Vimeux, F., Frankenberg, C., Noone, D., & Worden, J. Understanding the sahelian water budget through the isotopic composition of water vapor and precipitation. Journal of Geophysical Research Atmospheres, 2010, 115(D24), 9-12.

Rokotyan, N. V., Zakharov, V. I., Gribanov, K. G., Schneider, M., Bréon, F.-M., Jouzel, J., Imasu, R., Werner, M., Butzin, M., Petri, C., Warneke, T., and Notholt, J. A posteriori calculation of δ18O and δD in atmospheric water vapour from ground-based near-infrared FTIR retrievals of $H_2{}^{16}O$, $H_2{}^{18}O$, and $HD^{16}O$. Atmospheric Measurement Techniques, 2014, 7(8): 2567-2580.

Ross R J, Elliott W P. Tropospheric water vapor climatology and trends over North America: 1973-93. Journal of Climate, 1996, 9(12): 3561-3574.

Scheepmaker, R. A., Frankenberg, C., Deutscher, N. M., Schneider,M., Barthlott, S., Blumenstock, T., Garcia, O. E., Hase, F.,Jones, N., Mahieu, E., Notholt, J., Velazco, V., Landgraf, J., and Aben, I. Validation of SCIAMACHY HDO/H_2O measurements using the TCCON and NDACC-MUSICA networks. Atmospheric Measurement Techniques, 2015, 8(4):1799-1818.

Schneider M, Yoshimura K, Hase F, and T. Blumenstock. The ground-based FTIR network's potential for investigating the atmospheric water cycle. Atmospheric Chemistry & Physics, 2010, 9(6):3427-3442.

Schneising, O., Bergamaschi, P., Bovensmann, H., Buchwitz, M., Burrows, J. P., Deutscher, N. M., Griffith, D. W. T., Heymann, J., Macatangay, R., Messerschmidt, J., Notholt, J., Rettinger, M., Reuter, M., Sussmann, R., Velazco, V. A., Warneke, T., Wennberg, P. O., and Wunch, D. Atmospheric greenhouse gases retrieved from SCIAMACHY: comparison to ground-based FTS measurements and model results. Atmospheric Chemistry and Physics, 2012, 12(3): 1527-1540.

Soden B J, Huang X. The radiative signature of upper tropospheric moistening. Science, 2005, 310(5749):841-4.

Steen-Larsen, H. C., Johnsen, S. J., Masson-Delmotte, V., Stenni, B., Risi, C., Sodemann, H., Balslev-Clausen, D., Blunier, T., Dahl-Jensen, D., Ellehoj, M. D., Falourd, S., Grindsted, A., Gkinis, V., Jouzel, J., Popp, T., Sheldon, S., Simonsen, S. B., Sjolte, J., Steffensen, J. P., Sperlich, P., Sveinbjörnsdóttir, A. E., Vinther, B. M., and White, J. W. C. Continuous monitoring of summer surface water vapor isotopic composition above the Greenland Ice Sheet. Atmospheric Chemistry and Physics, 2013, 13(9): 4815-4828.

Stein, A. F., Draxler, R. R., Rolph, G. D., Stunder, B. J. B., Cohen, M. D., and Ngan, F. NOAA's HYSPLIT atmospheric transport and dispersion modeling system[J]. Bulletin of the American Meteorological Society, 2015, 96(12): 2059-2077.

Sun, W., Lin G. H., Chen S. P., and Huang J. H. Application of stable isotope techniques and keeling plot approach to carbon and water exchange studies of terrestrial ecosystems. Acta Phytoecologica Sinica, 2005, 29(5):851-862.

Toon G C. Telluric line list for GGG2014. TCCON data archive, hosted by the Carbon Dioxide Information Analysis Center, Oak Ridge National Laboratory, Oak Ridge, Tennessee, USA.

Tuinenburg O A, Hutjes R W A, Kabat P. The fate of evaporated water from the Ganges basin. Journal of Geophysical Research Atmospheres, 2012, 117(D1):815-817.

Vogelmann, H., Sussmann, R., Trickl, T., and Reichert, A. Spatiotemporal variability of water vapor investigated using lidar and FTIR vertical soundings above the Zugspitze. Atmospheric Chemistry and Physics, 2015, 15(6): 3135-3148.

Washenfelder, R., Toon, G., Blavier, J., Yang, Z., Allen, N., Wennberg, P., Vay, S., Matross, D., and Daube, B. Carbon dioxide column abundances at the Wisconsin Tall Tower site. Journal of Geophysical Research Atmospheres, 2006, 111(D22):5295-5305.

Wang W, Liu W, Zhang T. Continuous field measurements of δD in water vapor by open-path Fourier transform infrared spectrometry[C]//Photonics Asia. International Society for Optics and Photonics, 2012: 85621B-85621B-10.

Wang W, Tian T, Liu C, Sun Y, Liu W, Xie P, Liu J, Xu J, Morino I, Velazco V A, Griffith D W T, Notholt J, and Warneke T. Investigating the performance of a greenhouse gas observatory in Hefei, China. Atmos. Meas. Tech., 10, 1–17, 2017

Wei, Z., K. Yoshimura, A. Okazaki, K. Ono, W. Kim, M. Yokoi, and C. Lai, Understanding the variability of water isotopologues in near-surface atmospheric moisture over a humid subtropical rice paddy in Tsukuba, Japan, J. Hydrol., 2016, 533, 91–102, doi:10.1016/j.jhydrol.2015.11.044.

Wen, X.-F., Zhang S.-C., Sun X.-M., Yu G.-R., and Lee X. Water vapor and precipitation isotope ratios in Beijing, China. Journal of Geophysical Research: Atmospheres, 2010, 115(D1).

Williams, D. G., Cable W., Hultine K., J. C. B. Hoedjes, E. A. Yepez, V. Simonneaux, S. Er-Raki, G. Boulet, H. A. R. de Bruin, A. Chehbouni, O. K. Hartogensis, and F. Timouk. Evapotranspiration components determined by stable isotope, sap flow and eddy covariance techniques. Agricultural & Forest Meteorology, 2004, 125(3–4):241-258.

Worden, J. R., Noone, D., Bowman, K., Beer, R., Eldering, A., Fisher, B., Gunson, M., Goldman, A., Herman, R., Kulawik, S. S., Lampel, M., Osterman, G., Rinsland, C., Rodgers, C., Sander, S., Shephard, M., Webster, C. R., and Worden, H. Importance of rain evaporation and continental convection in the tropical water cycle, Nature, 445, 528–532, 2007.

Wunch, D., Toon, G. C., Blavier, J.-F. L., Washenfelder, R A., Notholt, J., Connor, B. J., Griffith, D. W. T., Sherlock, V., and Wennberg, P. O. The total carbon column observing network. Philosophical Transactions of the Royal Society of London A: Mathematical, Physical and Engineering Sciences, 2011, 369(1943): 2087-2112.

Wunch, D., Toon, G. C., Sherlock, V., Deutscher, N. M., Liu, X., Feist, D. G., and Wennberg, P. O. The Total Carbon Column Observing Network's GGG2014 Data Version. Carbon Dioxide Information Analysis Center, Oak Ridge National Laboratory, Oak Ridge, Tennessee, USA, 2015.

Yepez E A, Williams D G, Scott R L, and Lin G. Partitioning overstory and understory evapotranspiration in a semiarid savanna woodland from the isotopic composition of water vapor. Agricultural & Forest Meteorology, 2003, 119(1):53-68.

Yoshida, Y., Kikuchi, N., Morino, I., Uchino, O., Oshchepkov, S., Bril, A., Saeki, T., Schutgens, N., Toon, G. C., Wunch, D., Roehl, C. M., Wennberg, P. O., Griffith, D. W. T., Deutscher, N. M., Warneke, T., Notholt, J., Robinson, J., Sherlock, V., Connor, B., Rettinger, M., Sussmann, R., Ahonen, P., Heikkinen, P., Kyrö, E., Mendonca, J., Strong, K., Hase, F., Dohe, S., and Yokota, T. Improvement of the retrieval algorithm for GOSAT SWIR XCO_2 and XCH_4 and their validation using TCCON data. Atmospheric Measurement Techniques, 2013, 6(6):1533-1547.

Yoshimura, K., Kanamitsu, M., Noone, D., and Oki, T.. Historical isotope simulation using reanalysis atmospheric data. Journal of Geophysical Research Atmospheres, 2008, 113(113), e60941-e60941.

Zhou, M.-Q., Dils, B., Wang, P., Detmers, R., Yoshida, Y., O'Dell, C. W., Feist, D. G., Velazco, V. A., Schneider, M., and De Mazière, M., Validation of TANSO-FTS/GOSAT XCO2 and XCH4 glint mode retrievals using TCCON data from near-ocean sites. Atmos. Meas. Tech., 9, 1415–1430, 2016.

Geosci. Instrum. Method. Data Syst. Discuss., https://doi.org/10.5194/gi-2018-43
Manuscript under review for journal Geosci. Instrum. Method. Data Syst.
Discussion started: 3 December 2018

Geoscientific Instrumentation Methods and Data Systems
Open Access
Discussions

Table 1. The statistics of monthly averaged δD and surface temperature.

	Sep.	Oct.	Nov.	Dec.	Jan.	Feb.	Mar.	Apr.	May.	Jun.	Jul.	Aug.
δD (‰)	-126.89	-131.94	-209.71	-221.13	-257.86	-180.4	-107.65	-111.92	-113.66	-95.94	-69.52	-79.54
Variation amplitude of δD (‰)	117.5	172.46	168.64	186.38	392.17	213.66	182.29	118.7	155.85	87.76	67.9	93.78
Temperature(°C)	30.18	24.01	14.55	8.94	4.74	11.65	16.07	24.01	26.49	31.12	37.09	34.63
Variation amplitude of temperature (°C)	10.9	15	13.9	14.1	19.5	19.2	14.4	11.4	14.4	10.5	6.3	8

Geosci. Instrum. Method. Data Syst. Discuss., https://doi.org/10.5194/gi-2018-43
Manuscript under review for journal Geosci. Instrum. Method. Data Syst.
Discussion started: 3 December 2018

Geoscientific Instrumentation Methods and Data Systems
Open Access
Discussions

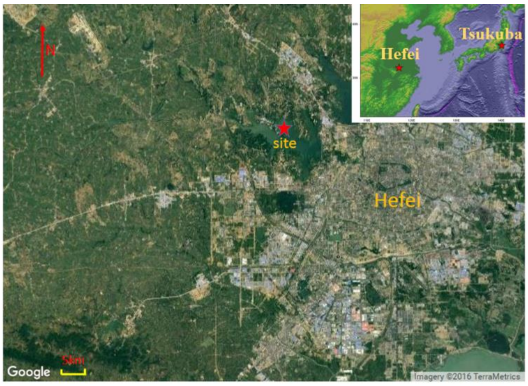

Figure1: Positions of Hefei and Tsukuba sites

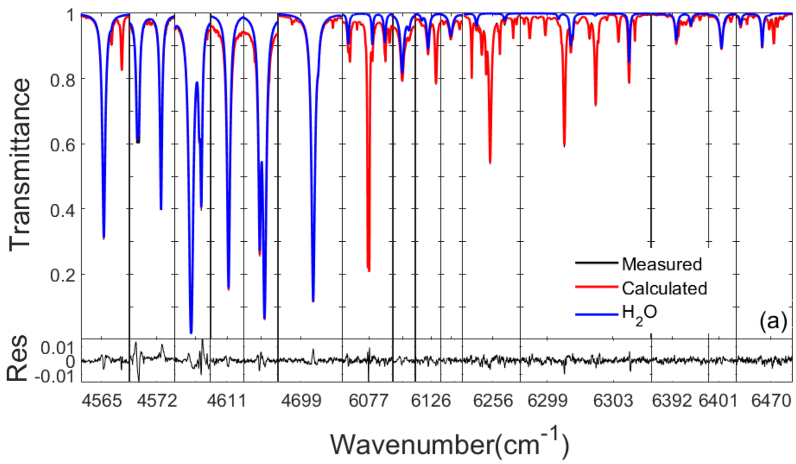

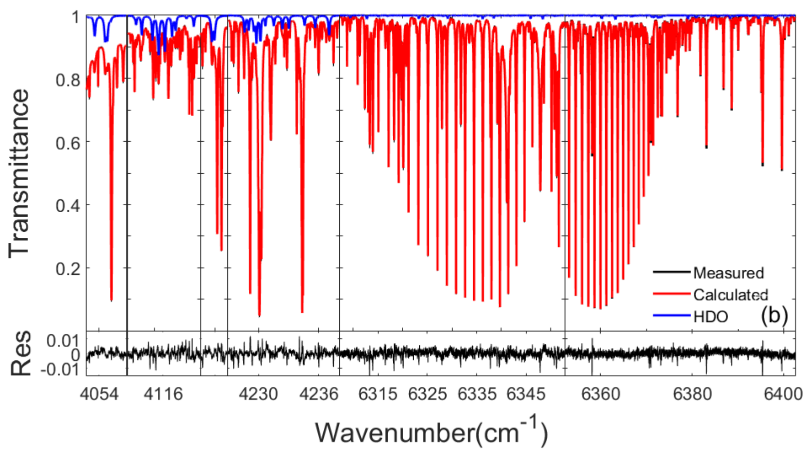

Figure 2: The spectral fitting of H_2O (a) and HDO (b). The black lines represent the measured spectra,the red lines represent the calculated spectra, the blue lines respesent the absorption signals for H_2O and HDO. The bottom panels are the spectra fitting residuals.

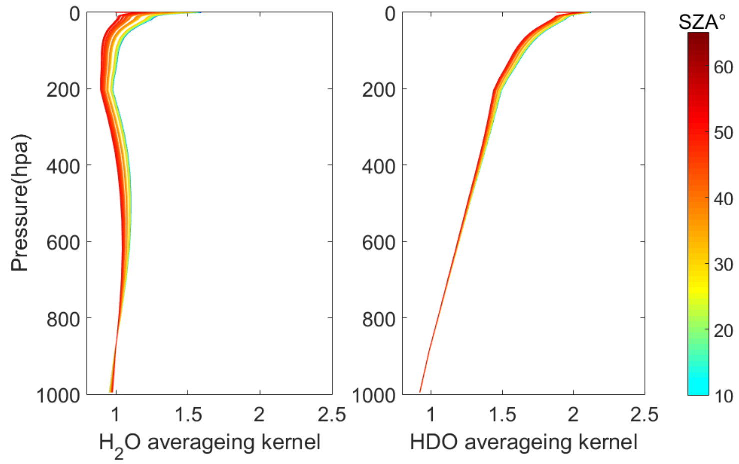

Figure 3: Column averaging kernels of H_2O and HDO

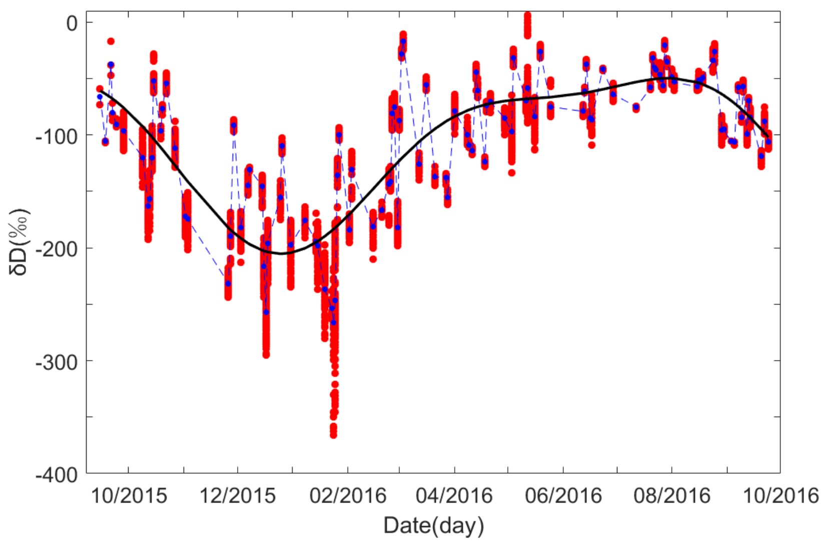

Figure 4: Time series of δD from September 2015 to September 2016 at Hefei site. The red points are the individual measurements, the blue points represent the daily averaged data, and the black line is the Fourier fitting line of time series.

Geosci. Instrum. Method. Data Syst. Discuss., https://doi.org/10.5194/gi-2018-43
Manuscript under review for journal Geosci. Instrum. Method. Data Syst.
Discussion started: 3 December 2018

Geoscientific Instrumentation Methods and Data Systems
Discussions
Open Access

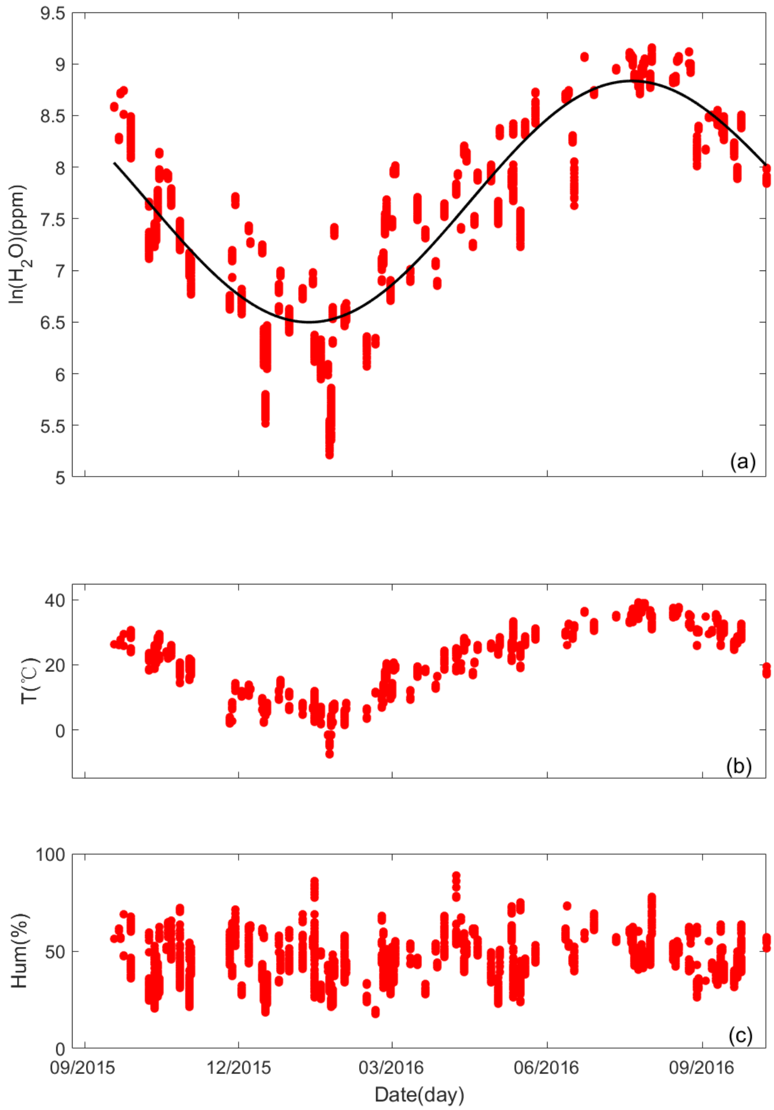

Figure 5: Time series of X_{H2O}, surface temperature and surface relative humidity from September 2015 to September 2016 at Hefei site. (a) Time series of X_{H2O} with the $\ln(X_{H2O})$ of Y axis, and the black line was fitted line; (b) Time series of surface temperature; and (c) Time series of surface relative humidity.

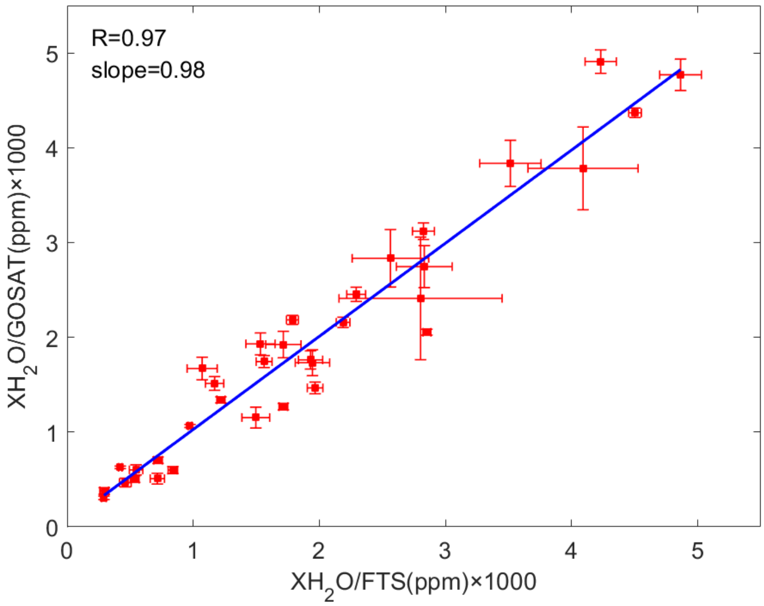

Figure 6: The scatter plot of X_{H2O} at Hefei site and the coincident GOSAT data

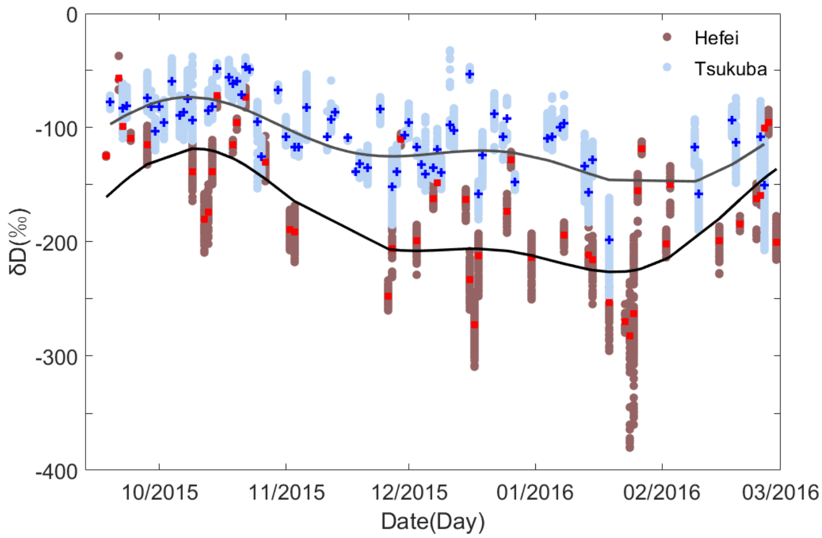

Figure 7: Time series of δD in Hefei and Tsukuba stations, respectively. The red and blue dots are daily averaged δD at Hefei and Tsukuba, the black lines are the Fourier fitting lines of time series for each site.

Geosci. Instrum. Method. Data Syst. Discuss., https://doi.org/10.5194/gi-2018-43
Manuscript under review for journal Geosci. Instrum. Method. Data Syst.
Discussion started: 3 December 2018

Geoscientific Instrumentation Methods and Data Systems
Discussions
Open Access

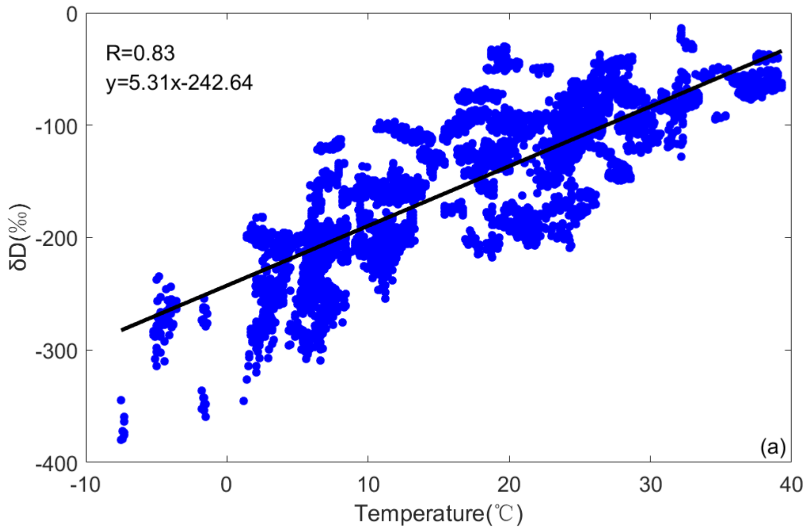

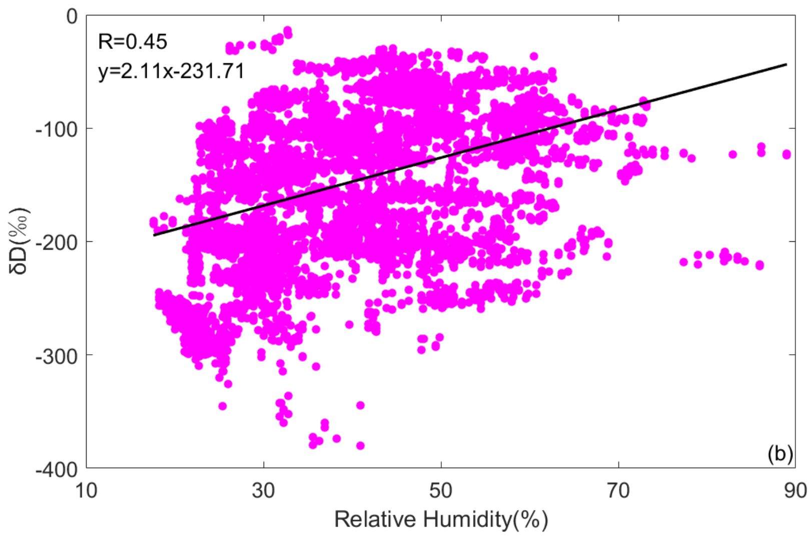

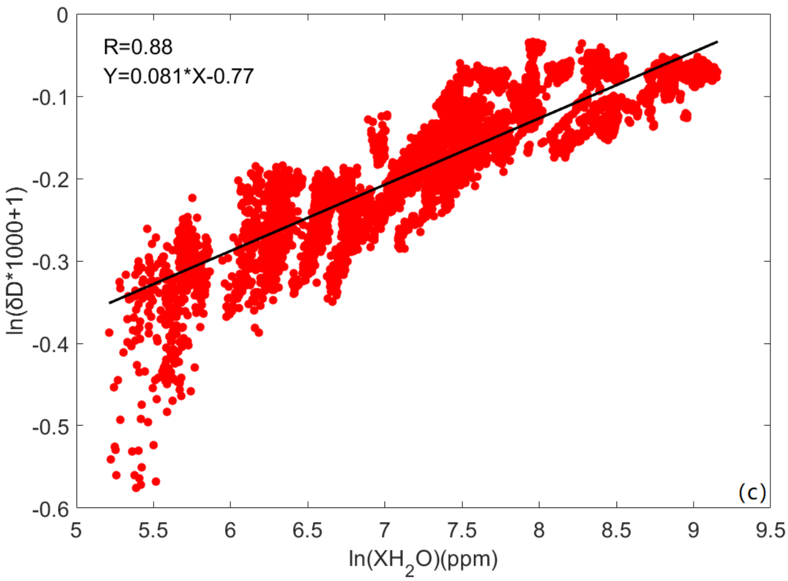

Figure 8: Relationship of the stable isotopes of water vapor with the meteorological parameters. (a). The relationship between δD and temperature. (b).The relationship between δD and relative humidity. (c). Scatter plots of ln(δD/1000+1) and ln(X_{H2O})

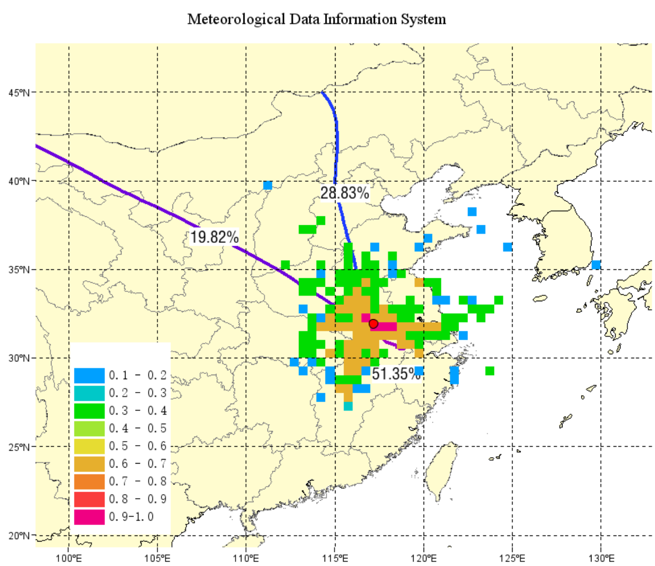

Figure 9: Cluster calculated of backward trajectories and the WPSCF of δD analysis at Hefei. The colourful area in the map denotes the potential sources regions calculated from the trajectory statistics.

Geosci. Instrum. Method. Data Syst. Discuss., https://doi.org/10.5194/gi-2018-43
Manuscript under review for journal Geosci. Instrum. Method. Data Syst.
Discussion started: 3 December 2018

Geoscientific Instrumentation Methods and Data Systems Discussions
Open Access

And the colourful line represent the cluster analysis result.

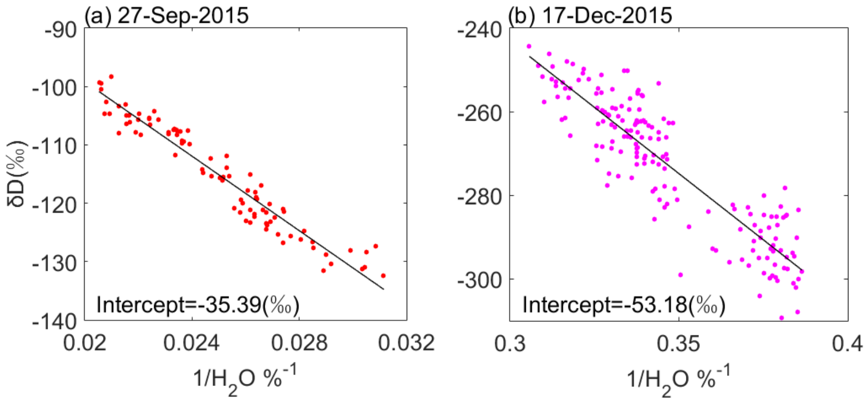

Figure 10: Keeling plots of measurements on October 27, 2015 and December 17, 2015.

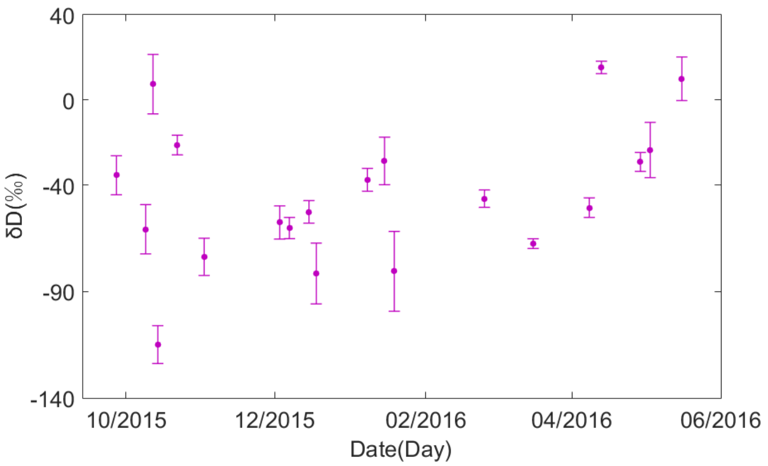

Figure 11: δD values of evapotranspiration during the measurement period. The error bars are standard deviations of value